Chemical Papers
https://doi.org/10.1007/s11696-020-01394-w

ORIGINAL PAPER

Electrochemical sensing of N-phenyl-1-naphthylamine using the MWCNT/β-CD through 'host scavenger–guest pollutant' mechanism

Vigneshkumar Ganesan[1] · Maniyazagan Munisamy[2] · Esakkimuthu Shanmugasundaram[1] · Krishnamoorthy Sivakumar[3] · Senthilvelan Sambandam[4] · Paramasivaganesh Kumaraswamy[5] · Stalin Thambusamy[1]

Received: 22 April 2020 / Accepted: 15 October 2020

Abstract

In this report, the synergistic effect of MWCNTs and β-cyclodextrin (β-CD) on glassy carbon electrode (GCE) for the electrochemical sensing of N-Phenylnaphthalen-1-amine (NPN) is demonstrated. The dual role of β-CD (i) as a modifier for MWCNTs, (ii) as scavenger host molecule for entrapping NPN guest molecule is also demoed through material characterization and sensing techniques. The functionalization of β-CD with MWCNTs is corroborated using spectral and XRD techniques. The emplacement of β-CD molecules in between the nanotube walls is affirmed through surface morphological and dispersion investigations. The physically modified β-CD/MWCNTs/GCE electrode possesses good dispersibility, acceptable stability, fast response, selectivity, the sensitivity of 10^{-6} M, the low detection limit of 15×10^{-9}, and high recovery value of 100% in real samples.

Keywords Multiwall carbon nanotubes · β-cyclodextrin · N-phenyl-1-naphthylamine · Electrochemical sensor

Introduction

Besides the two specific nanoscopic characteristics; strong redox capacity and large surface area, cost-effectiveness has progressed multi-wall carbon nanotubes (MWCNTs) as ineluctable by replacing established expensive materials (Canbay and Akyilmaz 2014; Sun et al. 2011) for electrochemical sensing (Yang et al. 2007; Kim et al. 2009; David et al. 2015; Mei et al. 2019; Güleşen et al. 2019). High electrical conductivity originating from the nanotopographic property of MWCNTs enhances the current response and detection efficiency of sensory material (Frankland et al. 2002; Yanez-Sedeno et al. 2010; Gooding 2005; Aliakbarinodehi et al. 2015). Despite high electron transfer efficiency, bundling and aggregation of pristine MWCNTs due to intrinsic van der Waals interaction reduce the solubility (Aragay et al. 2011), thereby restraining its utility in sensing application.

Functionalized multi-wall carbon nanotubes (f-MWCNTs) showed better sensing behavior (Du et al. 2010; Filik et al. 2019) than pristine MWCNTs. Functionalization of MWCNTs is generally achieved through covalent modifications: dodecylbenzene sulfonate, and Nafion (Wang and Yue 2017) or non-covalent modifications: amino (-NH2) (Wei et al. 2012), thiol groups (-SH) (Li et al. 2016), amino acids (Fu et al. 2013), cyclam, calixarene, crown-ether (Goubert-Renaudin et al. 2009; Dernane et al. 2013; Rouis et al. 2013; Parat et al. 2006) and βCD (Gaichore and Srivastava 2013; Alam et al. 2018; Yi et al. 2016; Aryal and Jeong 2019; Chambers et al. 2003; Luque De Castro et al. 2008) to overcome the aforementioned limitations.

✉ Stalin Thambusamy
drstalin76@gmail.com; stalin.t@alagappauniversity.ac.in

[1] Department of Industrial Chemistry, Alagappa University, Karaikudi, Tamilnadu 630003, India

[2] Department of Nanotechnology and Advanced Materials Engineering, College of Engineering, Sejong University, Gwangjin-gu, Seoul 05006, Korea

[3] Department of Chemistry, Faculty of Science, Sri Chandrasekharendra Saraswathi Viswa Mahavidyalaya University (SCSVMV University), Kanchipuram, Tamilnadu 631561, India

[4] Department of Chemistry, Annamalai University, Annamalainagar, Chidambaram, Tamilnadu 608002, India

[5] Department of Chemistry, Arumugam Pillai Seethai Ammal College, Thirupputtur, Sivagangai, Tamilnadu 630211, India

Published online: 24 October 2020

MWCNTs functionalized with macromolecules such as β-CD result in a new material exhibiting the property of both (MWCNTs and β-CD) compounds which could be synergistically useful in the sensing process (Del Valle 2004; Rahemi et al. 2012, 2013; Shen and Wang 2009; Niu et al. 2019; Gao et al. 2014, 2016). f-MWCNTs accommodate and hold the uniformly distributed β-CD molecules by non-covalent interactions: hydrogen bonding, and van der Waals forces between walls. The MWCNTs/β-CD material which generates a large surface area on the electrode through poriferous interspaces shows signal enhancement, rapidity in response, quick electrode kinetics, and low detection limit in the electrochemical sensing.

Noteworthy, numbers of reports are available in the literature specific to understand the contribution of MWCNTs and β-CD to the synergistic effect in the sensing process (Del Valle 2004; Rahemi et al. 2012, 2013; Shen and Wang 2009; Niu et al. 2019; Gao et al. 2014, 2016). f-MWCNTs kicks in the surface area of the electrode, thereby increasing the loading efficiency of pollutants, accelerate electron transfer, amplifies signal due to the high conductivity of nanotubes. Hydrophobic hallow space in the center of β-CD acts as a scavenger (host molecule) for the entrapment of pollutant (guest molecule) into the cavity with a sterically stable fit. Thus, the MWCNTs/β-CD material posited on the electrode renders a highly active surface for the redox process for the effective quantification of pollutants in low concentration.

N-phenyl-1-naphthylamine (NPN) enters into the environment through the vulcanization process, leakage of lubricating oils, and from the discarded rubber products (Khang et al. 2019; Weiss et al. 2013). Accumulation of NPN in the environment and exposure could cause lung and kidney cancer in mice (Wang et al. 1984), and imbalances the metabolism (Rosenberg 1983). Hence, developing facile analytical techniques for the effective detection of NPN is mandatory.

However, to the best of our knowledge electrochemical sensing of NPN has not been reported and this is the first report on the detection of NPN using modified (with f-MWCNT/β-CD) GCE. β-CD plays a dual role: (1) as a modifier for MWCNTs, (2) as a scavenger (host molecule) for entrapping NPN (guest molecule) which shows a greater affinity towards NPN with through host–guest interaction (Maniyazagan et al. 2014).

Materials and methods

Materials

N-Phenyl-1-naphthylamine (NPN) was purchased from Fisher Scientific, India, β-Cyclodextrin (β-CD), dimethylacetamide (DMA) and sodium nitrite ($NaNO_2$) obtained from the Sigma-Aldrich and used directly without further purification. Spectrograde solvents obtained from the Merck, MWCNT (95%) were obtained from SRL, India. Phosphate buffer solutions (PBS) in the pH range of 3–8 were prepared using KH_2PO_4 and K_2HPO_4. pH was adjusted using hydrochloric acid (HCl 37%) and NaOH.

Methods

Functionalization of MWCNTs

First, MWCNTs are oxidized in a hot solution of HNO_3 and H_2SO_4 (1:3 by volume) at 90 °C for 6 h to remove the impurities and to generate the surface, functional groups. After cooling and making to ambient temperature, the MWCNTs were centrifuged and washed to neutral. The prepared material was washed with distilled water and then dried. 200 mg of β-CD was mixed with 100 mg processed MWCNTs, ultrasonicated and the resulting suspension was cooled to room temperature, filtered through 0.2 µm pore size polytetrafluoroethylene membrane. The filtrate was washed three times with water, followed by drying at 50 °C for 48 h.

Characterization of MWCNTs and surface morphology studies

The functionalized MWCNTs f-MWCNTs (Oxidized) were characterized using FTIR and Raman spectroscopy. FTIR spectra were measured on a Nicolet 380 FTIR spectrometer with 4 cm^{-1} resolution and 32 scans between wave number 4000 cm^{-1} and 400 cm^{-1}. Samples were prepared as KBr disks with 1 mg of sample in 100 mg of KBr. FT-Raman spectra were measured on a Bruker RFS 27 stand-alone FT-Raman spectrometer with 2 cm^{-1} resolution and the spectral range was 4000–200 cm^{-1}. Fluorescence measurements were recorded using JASCO spectrofluorimeter, model FP 8200. XRD patterns were recorded Xpert PRO PANalytical diffractometer at 298 K. Monochromatic Cu Kα-radiation was obtained with a Nickel-filtration, and a system diverging and receiving slides were 1° and 0.2 mm, respectively. The patterns were recorded on a quartz plate at a tube voltage of 40 kV and a current of 30 mA over a 2θ range of 5–45° using a step size of 0.05° at a scan speed of 10 S/step. SEM micrographs were recorded using a FEI QUANTA 200. The powders were previously fixed on a brass stub using double-sided adhesive tape and then were made electrically conductive by coating, in a vacuum with a thin layer of gold for the 30 s and 30 W. The pictures were taken at an excitation voltage of 15 kW, 20 kW or 30 kW, and a magnification of 1080, 1200, 1400, or 2000x.

Electrochemical studies

The electrochemical studies were carried out using a conventional three-electrode cell. Here, we have used platinum as the counter electrode, and silver and silver chloride as the reference electrode. A glassy carbon electrode (GCE) modified with f-MWCNT was used as a working electrode. All electrochemical measurements were carried out with the aid of an Auto lab electrochemical analyzer (GPES software). All measurements were taken under the presence of a nitrogen atmosphere at room temperature.

Electrode modifications

The GCE is first polished to a mirror-like surface with 0.3 µm and 0.05 µm α-alumina slurries and then ultrasonicated for 1 min in ethanol and water successively. A quantity of 1 mg of f-MWCNT was dissolved in ethanol/xylene solution (3:1 wt/wt) by ultrasonication. Then, 10 µl of this solution was introduced over the GCE, left for 30 min to get dried at 60 °C. The modified electrode was kept at room temperature when not in use.

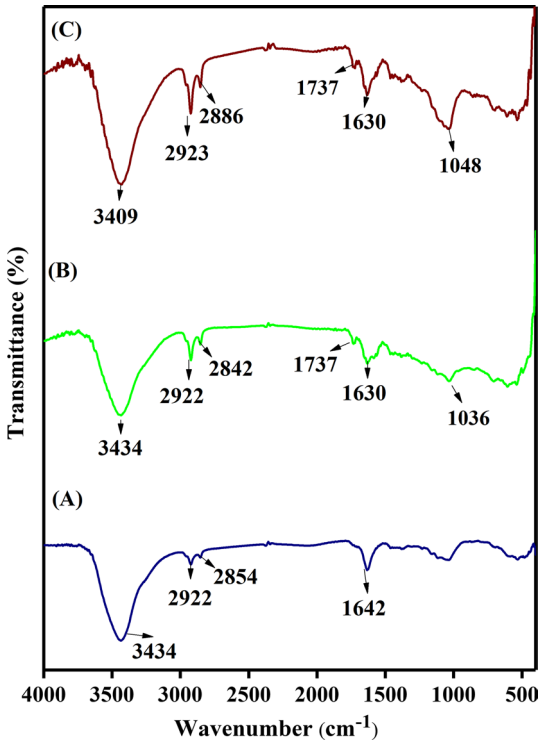

Fig. 1 FT-IR spectra of pristine MWCNT (**a**), f-MWCNT (**b**) and f-MWCNT/β-CD in KBr (**c**)

Results and discussion

FTIR spectral analysis

Figure 1 shows the FTIR spectra of pristine MWCNTs, f-MWCNTs (oxidized), and f-MWCNT/β-CD. The Pristine and f-MWCNTs spectra have the same range of O–H and C–H stretching frequency which appears at 3434 cm^{-1} and 2922 cm^{-1}. But, the f-MWCNT/β-CD matrix spectra shifted to 3409 cm^{-1}. The peak 1737 cm^{-1} indicates the carbonyl(C = O) group present in the f-MWCNTs (oxidized) and f-MWCNT/β-CD matrix/composite. Significant peak shift values and increase in the intensity of C–O peak at 1048 cm^{-1} in the f-MWCNT/β-CD spectrum confirms the incorporation of β-CD into the MWCNTs. The detailed list of peaks and their assigned functional groups is summarized in Table 1.

Raman spectroscopic analysis

Raman spectroscopy is contributing to point out the data on the molecular structure and crystallinity of both f-MWCNTs and f-MWCNTs/ β-CD of a composite/matrix material by the meticulous evaluation of the band frequencies. Alteration in f-MWCNT and the β-CD matrix band spectral report has also been propounding their loading characterization. Predominantly, a shift of the G band was found depending on the concentration of MWCNT. The Raman spectra of pristine MWCNT, f-MWCNT, f-MWCNT/β-CD (Fig. 2) show D and G bands at 1348 cm^{-1} and 1582 cm^{-1}, respectively.

The intensity ratio of these bands (I_D/I_G) is in the ratio of the amorphous/disordered carbon (sp^3) relative to that of the graphitic carbon (sp^2). In the functionalization studies, higher I_D/I_G values indicate a greater extent of C = C rupture implying higher covalent functionalization on the surface of the CNTs (Wang et al. 2018). I_D/I_G value of the f-MWCNT is larger than that of oxidized and pristine MWCNTs, which implies the successful incorporation of β-CD in between the walls of the MWCNTs.

Fluorescence spectroscopic analysis

The fluorescence peaks observed at 377 nm and 403 nm on exciting at 248 and 253 nm, respectively, infer that the emission intensity of f-MWCNT and f-MWCNT/β-CD is remarkably higher when compared to the pristine MWCNTs (Fig. 3). The emission intensity ratio of pristine MWCNT, oxidized f-MWCNT, and f-MWCNT/β-CD at 377 nm and 403 nm is 0.65, 0.75, and 0.92, respectively. These results indicate that the numbers of disordered carbons were increased after the functionalization of the MWCNT with β-CD (Teoh et al. 2018; Wang et al. 2018).

Table 1 Fourier transform infrared interpretation of the pristine, f-MWCNTs and f-MWCNTs/β-CD

Type of IR band or type of vibration	Pristine MWCNT (cm^{-1})	f-MWCNT (cm^{-1})	f-MWCNT/β-CD (cm^{-1})
O–H Stretching	3409	3434	3434
C–H Asymmetry Stretching	2922	2922	2923
C–H symmetry Stretching	2854	2842	2886
C = O Stretching	–	1737	1737
C = C Stretching	1642	1630	1630
C–O Stretching	–	1036	1048

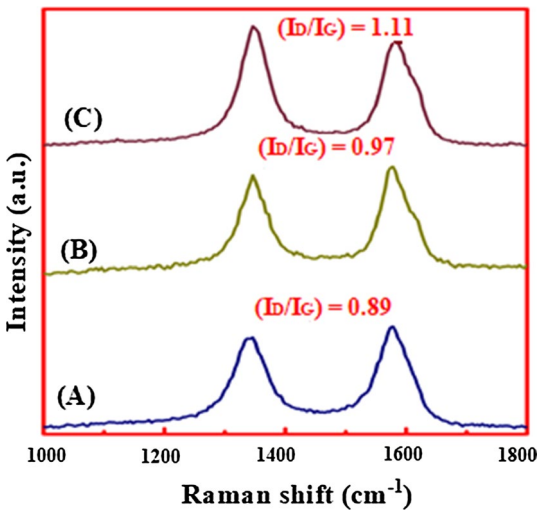

Fig. 2 FT-Raman spectra of pristine MWCNT (**a**), f-MWCNT (**b**) and f-MWCNT/β-CD (**c**)

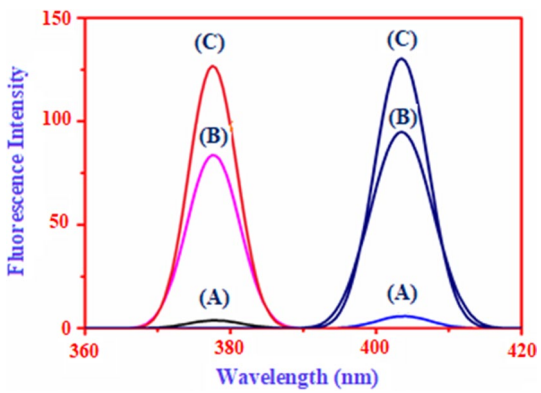

Fig. 3 Fluorescence emission spectra of pristine MWCNT (**a**), f-MWCNT (**b**) and f-MWCNT/β-CD in 1:1 Ethanol/xylene (**c**)

X-ray diffraction analysis

XRD pattern of pristine MWCNTs, f-MWCNTs, β-CD/f-MWCNTs composite is shown in Fig. 4a–d; the Fig. 4a pattern exhibits an intense diffraction peak around 2θ ~ 24,

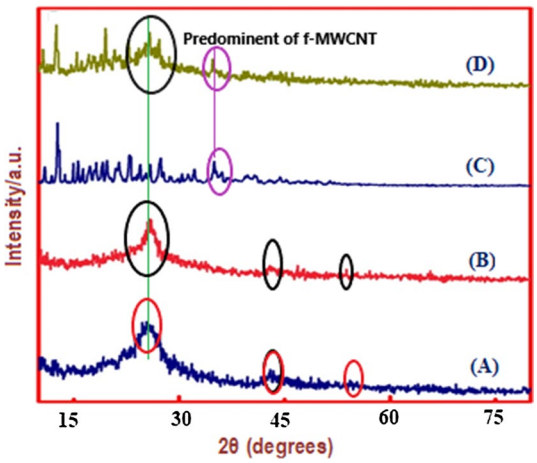

Fig. 4 X-ray diffraction (XRD) patterns of pristine MWCNT (**a**), Oxidized f-MWCNT (**b**), β-CD (**c**) and f-MWCNT/β-CD (**d**)

low intense diffraction peaks around 43 and 53 which are assigned to diffraction patterns of expected graphite, respectively. This result designates that MWCNTs are good conditionally graphitized. It is noticed from the XRD pattern that impurities and metal particles do not appear in the MWCNTs. Figure 4b shows the X-ray patterns for MWCNT oxidized with HNO_3. Activation can be done with the formation of functional groups at the sidewalls and the end of the tubes, which makes them more reactive. The combination of the f-MWCNTs electrocatalytic activity with the known advantages of other molecules (β-CD; Fig. 4c) gives a very important alternative for new electroanalytical behaviors. Here, β-CD usually involves the formation of inclusion complexes; also, it is used as recognition agents and to study the adsorption behavior related to electrode interactions. For these essential electrochemical properties of f-MWCNTs with the β-CD matrix, XRD is indicated as shown in Fig. 4d (Mohammadi and Veisi 2018).

Surface morphology analysis

SEM images are presented in Fig. 5, and the morphology of f-MWCNT, β-CD, and f-MWCNT/β-CD is described. The

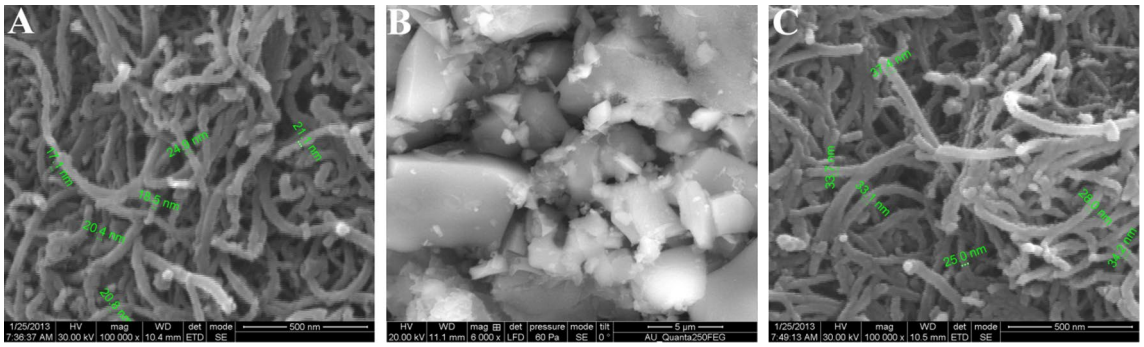

Fig. 5 Photographs by scanning electron microscopy of f-MWCNT (**a**), β-CD (**b**) and f-MWCNT/β-CD (**c**)

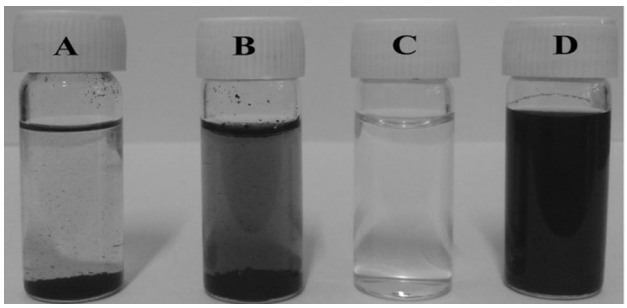

Fig. 6 Dispersion stability of samples in ethanol/xylene after 48 h from the sonication: Pristine MWCNT (**a**), f-MWCNT (**b**), β-CD (**c**) and f-MWCNT/β-CD (**d**)

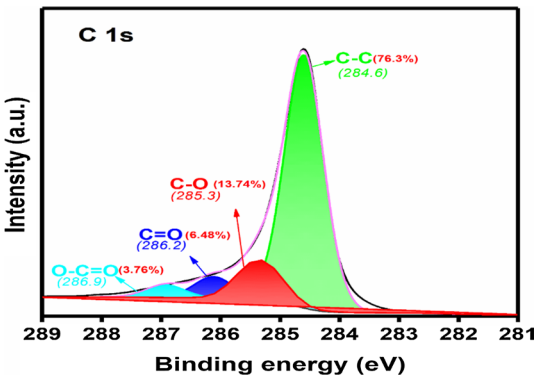

Fig. 7 XPS spectra of the f-MWCNT@β-CD composite and the assigned bonds

variation in morphology between oxidized f-MWCNTs and f-MWCNT/β-CD is evident. The uniform surface of the formation of compact 3D shapes in f-MWCNT (Fig. 5c) with an increased tube diameter of 20 nm without damaging the integrity of the MWCNT patterns (Prasad Aryal and Kyung Jeong 2019). The uniformity in the surface and increased diameter of f-MWCNT are suggestive indicators for the stability of f-MWCNT and the integration of β-CD molecules between the walls of nanotubes (Shao et al. 2010). Functionalization of β-CD is further confirmed by dispersion experiments in ethanol/xylene solution (3:1 wt/wt) on pristine MWCNT, oxidized MWCNT, and f-MWCNT (Fig. 6). After 24-h sonication, pristine MWCNT and oxidized MWCNT settle down, whereas the f-MWCNT remains stably dispersed even after sonication for > 48 h (Moghaddari et al. 2018).

XPS analysis

The X-ray Photoelectron Spectroscopy (XPS) survey and the signals are shown in Fig. 7. Here, the elements present and absence of the β-CD and f-MWCNT peaks in the respective composite have been discussed. The C–C and C–O peaks are present in the β-CD and f-MWCNT materials due to their significant chemical structure. Here, the electrostatic interactions and the immobilization capability of f-MWCNTs are combined with the β-CD adsorption characteristics, a well-known phenomenon occurring onto carbon (Fig. 7). The C1s C–O peak at 285.3(13.74%) and the O–C–O peak at 286.9 (3.76%) are the attached hydroxyl linkage of β-CD. The C1s f-MWCNT peak position of C–C appears at 284.6(76.3%). The C = C peaks are absent in this composite. From this result, the driving forces for the f-MWCNTs and β-CD composites are created from van der Waals forces between MWCNTs and β-CD and/or hydrogen bonding interaction between adjacent β-CD molecules. β-CD is sandwiched between the walls of f-MWCNTs and attaching of β-CD only to the outer shell of f-MWCNTs. This can also be verified by the above SEM observation of strong evidence of the driving forces (Kesong Liu et al. 2008). Furthermore, this composite is used to adjust the electrode in order to detect the NPN and the mechanism can be proposed.

Electrochemical sensing of NPN

Figure 8 depicts the CVs of NPN on different electrodes; bare GCE, β-CD/ GCE, f-MWCNTs/GCE,

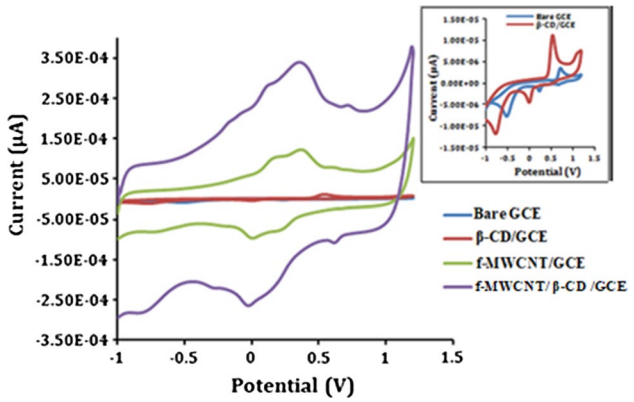

Fig. 8 Cyclic voltammograms of (0.1 mM) solutions of NPN at GCE (**a**), β-CD/GCE (**b**), f-MWCNT/GCE (**c**) and f-MWCNT/β-CD/GCE (**d**) in pH 7.4 phosphate buffer electrolyte. Scan rate: 50 mV s^{-1}

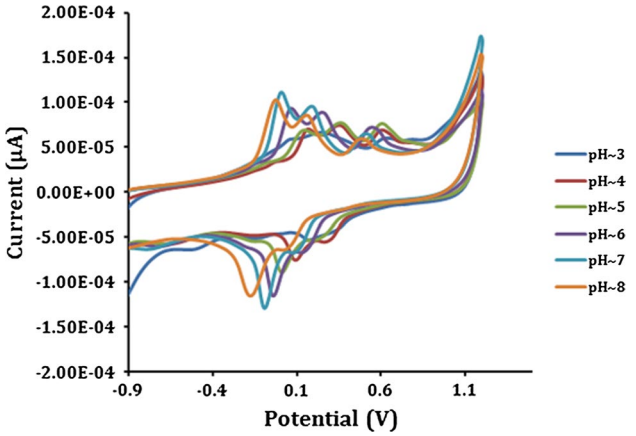

Fig. 9 Cyclic voltammograms of NPN (0.1 mM) at the GCE electrode at different PBS 3.0 to 8.0. Insert: the plot EP versus pH. Scan rate: 50 mV s^{-1}

f-MWCNTs/β-CD/GCE in 0.1 M PBS (pH ~ 7.4) containing 0.1 mM NPN. A pair of well-defined redox peaks of the NPN was observed within the potential window from − 1.5 to 1.5 V revealing that the NPN underwent a quasi-reversible redox process on the electrode. The peak currents of NPN are modest on bare GCE, β-CD/ GCE, f-MWCNTs/GCE, whereas it remarkably increased for the modified (with f-MWCNT) electrode; f-MWCNTs/β-CD/GCE can be attributed to the entrapment of NPN (guest pollutant) into the cavity of β-CD (scavenger host) (Sivakumar et al. 2013). The peak currents of NPN on different types of electrodes are increasing in the order: bare GCE < β-CD/GCE < f-MWCNTs/GCE < f-MWCNTs/β-CD/GCE. The synergistic contribution of MWCNTs and β-CD yields high peak currents for f-MWCNTs/β-CD/GCE. That is, (1) f-MWCNTs kicks in the surface area of the electrode, thereby raising the loading area for NPN, accelerates electron transfer, and results in amplification of peak current, (2) the pollutant NPN entraps into the β-CD cavity with a sterically stable fit through host–guest mechanism (Maniyazagan et al. 2014). These results indicate that the f-MWCNTs/β-CD/GCE has potential sensitivity towards NPN and hence, it has promising applications in the electrochemical detection of NPN.

pH optimization

To identify the optimum pH for sensing experiments, CVs of NPN on bare GCE were recorded over a range of pH 3.0–8.0 (Fig. 9).

It is found that the peak potential and peak current are dependent on the pH. The peak currents of the NPN increased with a negative shift of peak potential for raising pH 3.0–7.0, whereas the peak current decreases for pH > 8. Hence, pH 7.4 was chosen for further investigations.

Effect of the scan rate study

Figure 10 clearly shows that the scan rate had a prominent influence on the anodic and cathodic peak currents of NPN (1.0×10^{-4} mmol l^{-1}). The observed peak current of NPN is 100–600 mV s^{-1}. It is good linear; this is expressed as i_{pa} (μA) = $0.1092\nu^{1/2} - 0.3795$ with a correlation coefficient of $r^2 = 0.9919$. Hence, the anodic peak current response of the NPN on f-MWCNTs/β-CD/GCE was controlled by the mass diffusion, showing a diffusion-controlled process in the solution.

Sensing by differential pulse voltammetry

DPV was used for the detection of NPN under the optimized conditions. Figure 11 shows the DPV curves of NPN at f-MWCNTs/β-CD/GCE at various concentrations (0.05×10^{-6} to 0.35×10^{-6} M). The reduction peak currents are proportional to the concentration of the NPN in a wider range from 0.05×10^{-6} to 0.35×10^{-6} M. Excellent linear relationship ($r^2 = 0.992$) between peak current and different concentration of the NPN is observed. The proposed method has the lower detection limit (15×10^{-9}) and a wider linear range infers the potentiality of β-CD functionalized MWCNTs on GCE for the effective sensing of NPN.

Mechanism of the NPN detection

β-Cyclodextrin (Host) are good receptors for host–guest interactions. And, this is having many significant advantages over biological receptors, for example, good stability and lower-cost options for monitoring the pollutants (guest). Based on the host–guest interaction capability of β-CD combined with f-MWCNTs, the electrochemical detection of NPN (Scheme 1) is enhanced. This experiment

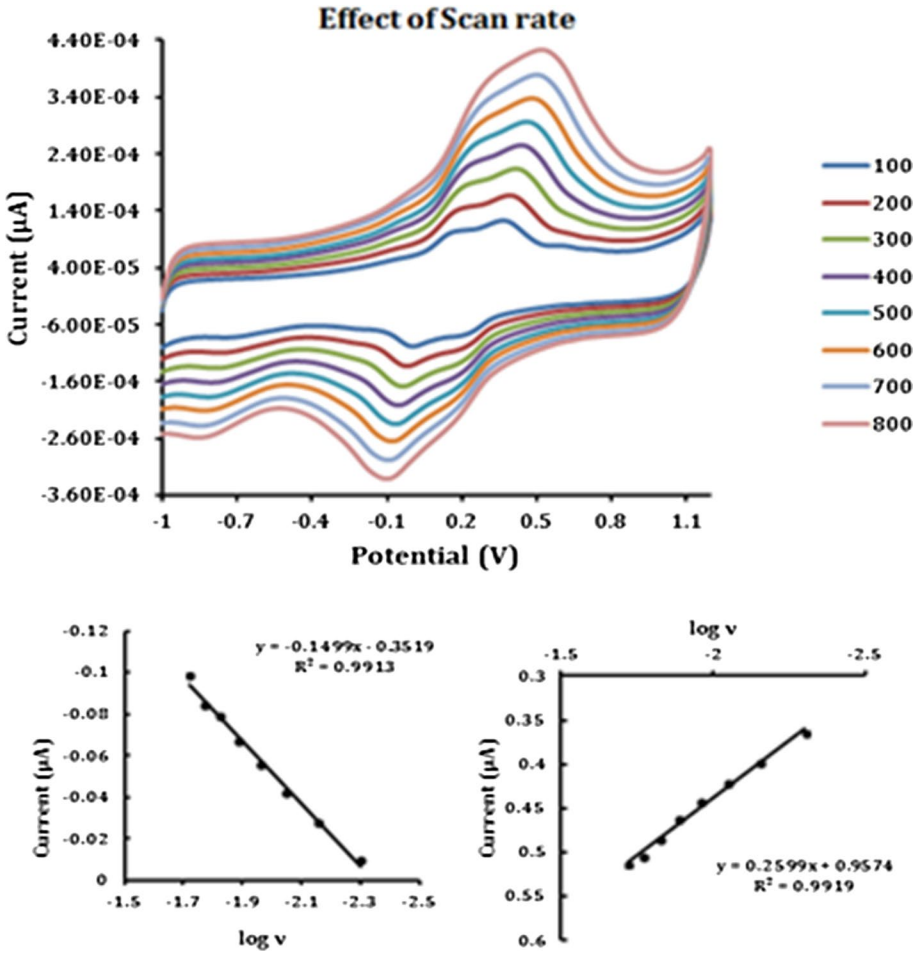

Fig. 10 Cyclic voltammograms of a 0.1 mM solution of NPN at f-MWCNT/ β-CD /GCE electrode in pH 7.4 PBS at different scan rates (**a**–**h**: 100–800 mV s^{-1}). The oxidation (**a**) and reduction peak currents versus the scan rate (**b**)

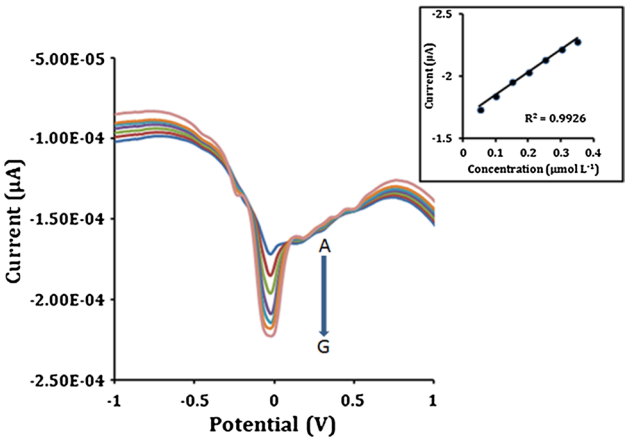

Fig. 11 Differential pulse voltammetry at MWCNT/β-CD/GCE in 0.1 M PBS of pH 7.4; Concentration of NPN 5.0×10^{-8} M (**a**), 1.0×10^{-7} M (**b**), 1.5×10^{-7} M (**c**), 2.0×10^{-7} M (**d**), 2.5×10^{-7} M (**e**), 3.0×10^{-7} M (**f**), 3.5×10^{-7} M (**g**). Insert: Plot of reduction peak current versus concentration of NPN

indicated that the NPN detection was done by electrochemical studies and a radical mechanism was explored. Here, no benzene or naphthyl group elimination occurred during the electrochemical studies; evidently, the free radical cation (1 electron transfer) is feasible. We propose the 1 electron transfer of NPN as shown in Scheme 2. In this Scheme, the radical is obtained by electrochemical oxidation of the NPN, and the mechanism is in good agreement with our electrochemical experimental results.

Here in Scheme 2, initially, N–H bond of the NPN molecule is broken. The molecule loses one hydrogen molecule and one electron and a nitrogen radical structure is formed. Then, the nitrogen radical is not stable. So, it involves resonance with neighbor carbon atom to form N = C. In addition, the radical transition of the aromatic system requires resonance. Finally, it's a carbon radical.

Application in real sample analysis

The proposed method with the above optimal conditions was used to determine the NPN in wastewater effluents collected from four different parts of Tamil Nadu, India. The determination was performed by the standard addition method. The execution of the chemical sensor was evaluated by the determination of the concentration of NPN present in the wastewater effluents. The experiment was first performed

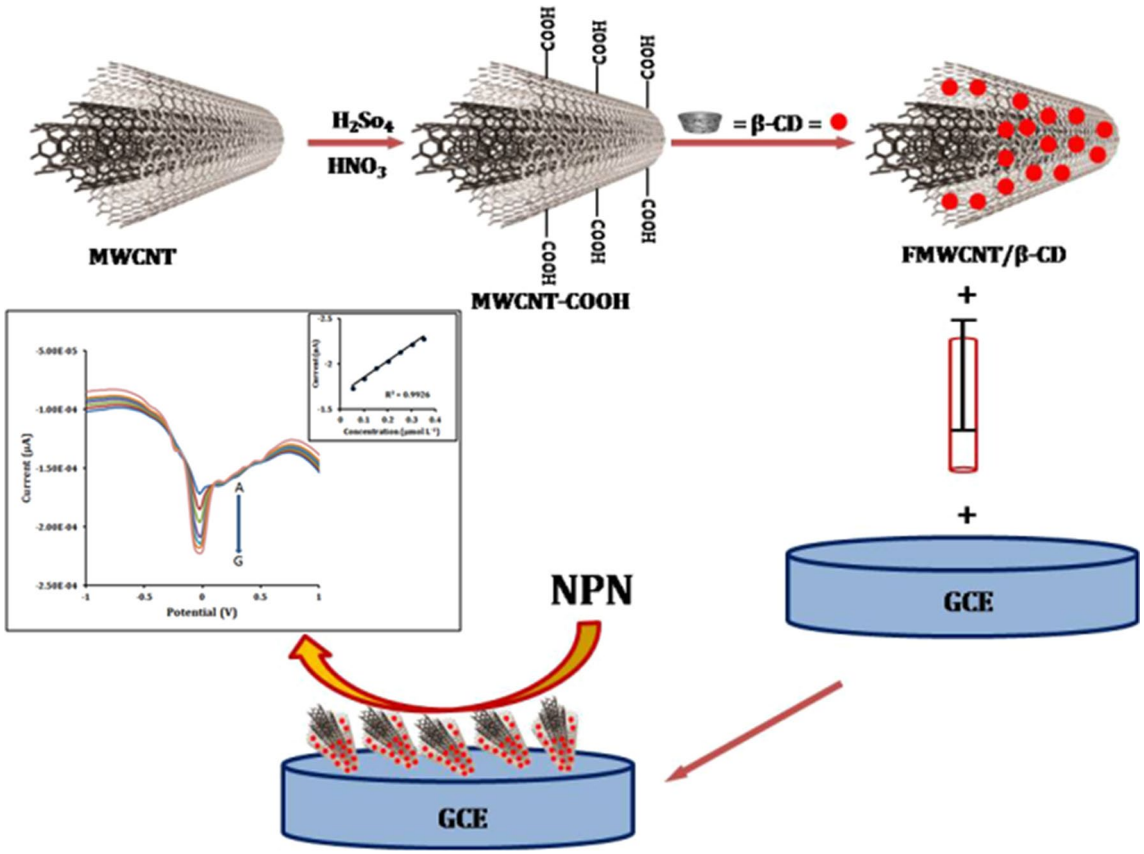

Scheme 1 The electrochemical sensor modified with the f-MWCNT/ β-CD matrix

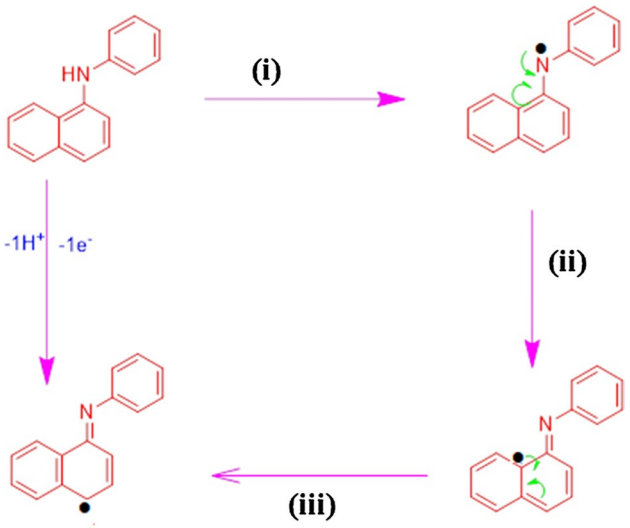

Scheme 2 The electrochemical sensor mechanism proposed by the NPN oxidation reaction with respect to 1 electron transfer is also shown

with wastewater with no NPN spiking. The wastewater was diluted 1:4 in PBS buffer solution (0.1 M, pH 7.4), and the experimental conditions were the same as the differential pulse Voltammetry used for interpretation of the calibration curve.

Here, no differences in the lower detection limit (15×10^{-9}) values obtained for the blank PBS buffer and for the incubated samples; it shows that not present in the NPN in the effluent. The sample was then spiked with NPN, the DPV measurement was carried out and then NPN determination was performed by the standard addition method. These analyses were performed for three times under the same conditions, and the results obtained are shown in Table 2. An average recovery value approaching 100% recovery infers

Table 2 Determination of NPN in waste water effluents

Samples	Found (μmol L^{-1})	Added (μmol L^{-1})	Found after added (μmol L^{-1})	Recovery ± SD (%)	Recovery (%)
1	–	5.0	5.10 ± 0.09	2.31	> 100
2	–	5.0	5.05 ± 0.11	3.17	> 100
3	–	5.0	4.90 ± 0.13	3.53	98.0
4	–	5.0	5.09 ± 0.08	2.16	> 100
					Approaching to 100% recovery

that β-CD functionalized MWCNTs on GCE is a promising and suitable material for the precise quantification of NPN in real samples.

Differential pulse voltammetry at MWCNT/β-CD/GCE in 0.1 M PBS of pH 7.4; Concentration of NPN in mm level.

Conclusions

In summary, the synergistic effects of MWCNTs; large surface area, and β-CD; affinity to host small molecule, are used for the detection of N-phenyl-1-naphthylamine by positing β-CD functionalized MWCNTs on GCE. The modified electrode β-CD/MWCNTs/GCE possesses good dispersibility, acceptable stability, fast response, selectivity, the sensitivity of 0.05×10^{-6} to 0.35×10^{-6} M, the low detection limit of 15×10^{-9}, and a high recovery value of 100% in real samples. The proposed method could be scaled up for relevant industrial applications.

Acknowledgements Dr. T. Stalin and G. Vigneshkumar, wish to thank for the financial support of RUSA-Phase 2.0 grant No.F. 24-51/2014-U, Policy (TNMulti-Gen), Dept. of Edn., Govt. of India, Dt. 09.10.2018.

Compliance with ethical standards

Conflict of interest The authors declare no competing financial interest.

References

Alam AU, Qin Y, Howlader MMR, Hu NX, Jamal Deen MJ (2018) Electrochemical sensing of acetaminophen using multi-walled carbon nanotube and β-cyclodextrin. Sens Actuators B 254:896–909. https://doi.org/10.1016/j.snb.2017.07.127

Aliakbarinodehi N, Taurino I, Pravin J, Tagliaferro A, Piccinini G, De Micheli G, Carrara S (2015) Electrochemical nanostructured biosensors: carbon nanotubes versus conductive and semi-conductive nanoparticles. Chem Pap. https://doi.org/10.1515/chempap-2015-0004

Aragay G, Pons J, Merkoçi A (2011) Recent trends in macro-, micro-, and nanomaterial based tools and strategies for heavy-metal detection. Chem Rev 111(5):3433–3458. https://doi.org/10.1021/cr100383r

Aryal KP, Jeong HK (2019) β-Cyclodextrin functionalization ofactivated Carbon-Carbon Nanotube composites and supramolecular recognition of Ascorbic acid. N Phys Sae Mulli 69:290–294.https://doi.org/10.3938/npsm.69.290

Canbay E, Akyilmaz E (2014) Design of a multiwalled carbon nanotube-Nafion-cysteamine modified tyrosinase biosensor and its adaptation of dopamine determination. Anal Biochem 444:8–15. https://doi.org/10.1016/j.ab.2013.09.019

Chambers G, Carroll C, Farrell GF, Dalton AB, McNamara M, PanhuisByrne MHJ (2003) Characterization of the interaction of gamma cyclodextrin with single-walled carbon nanotubes. Nano Lett 3(6):843–846. https://doi.org/10.1021/nl034181p

David IG, Florea MA, Cracea OG, Popa DE, Buleandra M, Iorgulescu EE, David V, Badea IA, Ciucu AA (2015) Voltammetric determination of B1 and B6 vitamins using a pencil graphite electrode. Chem Pap. https://doi.org/10.1515/chempap-2015-0096

Del Valle EMM (2004) Cyclodextrins and their uses: a review. Process Biochem 39(9):1033–1046. https://doi.org/10.1016/s0032-9592(03)00258-9

Dernane C, Zazoua A, Kazane I, Jaffrezic-Renault N (2013) Cadmium-sensitive electrode based on tetracetone derivatives of p-tert-butylcalix[8]arene. Mater Sci Eng C 33(7):3638–3643. https://doi.org/10.1016/j.msec.2013.04.049

Du D, Wang M, Cai J, Zhang A (2010) Sensitive acetylcholinesterase biosensor based on assembly of β-cyclodextrins onto multiwall carbon nanotubes for detection of organophosphates pesticide. Sens Actuators B146:337–341. https://doi.org/10.1016/j.snb.2010.02.053

Filik H, Avan AA, Yetimoğlu EK (2019) Multiwalled carbon nanotubes β- cyclodextrin modified electrode for electrochemical determination of bisphenol S in water samples. Russ J Electrochem 55(2):141–149. https://doi.org/10.1134/s1023193519010038

Frankland SJV, Caglar A, Brenner DW, Griebel M (2002) Molecular simulation of the influence of chemical cross-links on the shear strength of carbon nanotube-polymer interfaces. J Phys Chem B 106:3046–3048. https://doi.org/10.1021/jp015591+

Fu XC, Wu J, Li J, Xie CG, Liu YS, Zhong Y, Liu JH (2013) Electrochemical determination of trace copper (II) with enhanced sensitivity and selectivity by gold nanoparticle/single-wall carbon nanotube hybrids containing three-dimensional l-cysteine molecular adapters. Sens Actuators B Chem 182:382–389. https://doi.org/10.1016/j.snb.2013.02.074

Gaichore RR, Srivastava AK (2013) Voltammetric determination of nifedipine using a β-cyclodextrin modified multi-walled carbon nanotube paste electrode. Sens Actuators B Chem 188:1328–1337. https://doi.org/10.1016/j.snb.2013.08.052

Gao YS, Wu LP, Zhang KX, Xu JK, Lu LM, Zhu XF, Wu Y (2014) Electroanalytical method for determination of shikonin based on the enhancement effect of cyclodextrin functionalized carbon nanotubes. Chin Chem Lett 26(5):613–618. https://doi.org/10.1016/j.cclet.2014.11.032

Gao J, Zhang S, Liu M, Tai Y, Song X, Qian Y, Song H (2016) Synergistic combination of cyclodextrin edge-functionalized graphene and multiwall carbon nanotubes as conductive bridges toward enhanced sensing response of supramolecular recognition. Electrochim Acta 187:364–374. https://doi.org/10.1016/j.electacta.2015.11.073

Gooding JJ (2005) Nanostructuring electrodes with carbon nanotubes: a review on electrochemistry and applications for sensing. Electrochim Acta 50(15):3049–3060. https://doi.org/10.1016/j.electacta.2004.08.052

Goubert-Renaudin S, Moreau M, Despas C, Meyer M, Denat F, Lebeau B, Walcarius A (2009) Voltammetric detection of lead(II) using amide-cyclam- functionalized silica-modified carbon paste electrodes. Electroanalysis 21(15):1731–1742. https://doi.org/10.1002/elan.200904661

Güleşen M, Erkal-Aytemur A, Yavuz S, Akbulut A, Afşin Kariper İ, Üstündağ İ (2019) Evaluation of nanomanganese decorated typha tassel carbonaceous electrode: preparation, characterization, and simultaneous determination of Cd^{2+} and Pb^{2+}. Chem Pap 73(11):2869–2878. https://doi.org/10.1007/s11696-019-00839-1

Khang DQ, Lien TK, Hai LN, Minh DQ, Sy DT, Hai LH (2019) Study on preparation and properties of rubber blends based on nitrile butadiene rubber and chloroprene rubber. Macromol Symp 384:1800169. https://doi.org/10.1002/masy.201800169

Kim HS, Yoon SH, Kwon SM, Jin HJ (2009) pH-sensitive multiwalled carbonnanotube dispersion with silk fibroins. Biomacromol 10(1):82–86. https://doi.org/10.1021/bm800896e

Li X, Zhou H, Fu C, Wang F, Ding Y, Kuang Y (2016) A novel design of engineered multi-walled carbon nanotubes material

and its improved performance in simultaneous detection of Cd(II) and Pb(II) by square wave anodic stripping voltammetry. Sens Actuators B Chem 236:144–152. https://doi.org/10.1016/j.snb.2016.05.149

Liu K, Honggang Fu, Xie Y, Zhang L, Pan K, Zhou W (2008) Assembly of â-cyclodextrins acting as molecular bricks onto multiwall carbon nanotubes. J Phys Chem C 112:951–957. https://doi.org/10.1021/jp0756754

Luque de Castro MD, Ruiz-Jimenez J, Perez-Serradilla JA (2008) Lab-on-valve: a useful tool in biochemical analysis. Trends Anal Chem 27(2):118–126. https://doi.org/10.1016/j.trac.2008.01.004

Maniyazagan M, Mohandass S, Sivakumar K, Stalin T (2014) N-phenyl-1-naphthylamine/β-cyclodextrin inclusion complex as a new fluorescent probe for rapid and visual detection of Pd^{2+}. Spectrochim Acta Part A 133:73–79. https://doi.org/10.1016/j.saa.2014.04.183

Mei J, Ying Z, Sheng W, Chen J, Xu J, Zheng P (2019) A sensitive and selective electrochemical sensor for the simultaneous determination of trace Cd^{2+} and Pb^{2+}. Chem Pap. https://doi.org/10.1007/s11696-019-00942-3

Moghaddari M, Yousefi F, Ghaedi M, Dashtian K (2018) A simple approach for the sonochemical loading of Au, Ag and Pd nanoparticle on functionalized MWCNT and subsequent dispersion studies for removal of organic dyes: artificial neural network and response surface methodology studies. Ultrason Sonochem 42:422–433. https://doi.org/10.1016/j.ultsonch.2017.12.003

Mohammadi A, Veisi P (2018) High adsorption performance of β-cyclodextrin-functionalized multi-walled carbon nanotubes for the removal of organic dyes from water and industrial wastewater. J Environ Chem Eng 6(4):4634–4643. https://doi.org/10.1016/j.jece.2018.07.002

Niu X, Yang X, Mo Z, Guo R, Liu N, Zhao P, Liu Z, Ouyang M (2019) Voltammetric enantiomeric differentiation of tryptophan by using multiwalled carbon nanotubes functionalized with ferrocene and β-cyclodextrin. Electrochim Acta 297:650–659. https://doi.org/10.1016/j.electacta.2018.12.041

Parat C, Betelu S, Authier L, Potin-Gautier M (2006) Determination of labile trace metals with screen-printed electrode modified by a crown-ether based membrane. Anal Chim Acta 573–574:14–19. https://doi.org/10.1016/j.aca.2006.04.081

Prasad Aryal K, Kyung Jeong H (2019) Modification of β-cyclodextrin-carbon nanotube-thermally reduced graphite oxide by using ambient plasma for electrochemical sensing of ascorbicacid. Chem Phys Lett 730:306–311. https://doi.org/10.1016/j.cplett.2019.06.032

Rahemi V, Vandamme JJ, Garrido JMPJ, Borges F, Brett CMA, Garrido EMPJ (2012) Enhanced hosteguest electrochemical recognition of herbicide MCPA using a β-cyclodextrin carbon nanotube sensor. Talanta 99:288–293. https://doi.org/10.1016/j.talanta.2012.05.053

Rahemi V, Garrido JMPJ, Borges F, Brett CMA, Garrido EMPJ (2013) Electrochemical determination of the herbicide bentazone using a carbon nanotube β-cyclodextrin modified electrode. Electroanalysis 25:2360–2366. https://doi.org/10.1002/elan.201300230

Rosenberg A (1983) Microbial metabolism of N-Phenyl-1-naphthylamine in soil, soil suspensions, and aquatic ecosystems. Chemosphere 12(11–12):1517–1523. https://doi.org/10.1016/0045-6535(83)90082-6

Rouis A, Echabaane M, Sakly N, Dumazet-Bonnamour I, Ouada HB (2013) Electrochemical analysis of a PPV derivative thin film doped with ß-ketoimine calix [4]arene in the dark and under illumination for the detection of Hg^{2+} ions. Synth Met 164:78–87. https://doi.org/10.1016/j.synthmet.2013.01.005

Shao D, Sheng G, Chen C, Wang X, Nagatsu M (2010) Removal of polychlorinated biphenyls from aqueous solutions using β-cyclodextrin grafted multiwalled carbon nanotubes. Chemosphere 79(7):679–685. https://doi.org/10.1016/j.chemosphere.2010.03.008

Shen Q, Wang X (2009) Simultaneous determination of adenine, guanine and thymine based on β-cyclodextrin/MWNTs modified electrode. J Electroanal Chem 632(1–2):149–153. https://doi.org/10.1016/j.jelechem.2009.04.009

Sivakumar K, Hemalatha G, Parameswari M, Stalin T (2013) Spectral, electrochemical and docking studies of 5-indanol:β-CD inclusion complex. Phys Chem Liq 51(5):567–585. https://doi.org/10.1080/00319104.2012.760085

Sun CL, Chang CT, Lee HH, Zhou J, Wang J, Sham TK, Pong WF (2011) Microwave assisted synthesis of a core-shell MWCNT/GONR heterostructure for the electrochemical detection of ascorbic acid, dopamine, and uric acid. ACS Nano 5(10):7788–7795. https://doi.org/10.1021/nn2015908

Teoh WC, Yeoh WM, Mohamed AR (2018) Evaluation of different oxidizing agents on effective covalent functionalization of multiwalled carbon nanotubes. Fuller Nanotub Carbon Nanostruct 26(12):846–850. https://doi.org/10.1080/1536383x.2018.1508133

Wang T, Yue W (2017) Carbon nanotubes heavy metal detection with stripping voltammetry: a review paper. Electroanalysis 29(10):2178–2189. https://doi.org/10.1002/elan.201700276

Wang HW, Wang D, Dzeng RW (1984) Carcinogenicity of N-Phenyl-1-naphthylamine and N-Phenyl-2-naphthylamine in Mice. Cancer Res 44:3098–3100

Wang L, Tan Y, Wang X, Xu T, Xiao C, Qi Z (2018) Mechanical and fracture properties of hyperbranched polymer covalent functionalized multiwalled carbon nanotube-reinforced epoxy composites. Chem Phys Lett 706:31–39. https://doi.org/10.1016/j.cplett.2018.05.071

Wei Y, Yang R, Chen X, Wang L, Liu JH, Huang XJ (2012) A cation trap for anodic stripping voltammetry: NH3–plasma treated carbon nanotubes for adsorption and detection of metal ions. Anal Chim Acta 755:54–61. https://doi.org/10.1016/j.aca.2012.10.021

Weiss T, Bolt HM, Schlüter G, Koslitz S, Taeger D, Welge P, Brüning T (2013) Metabolic dephenylation of the rubber antioxidant N-phenyl-2-naphthylamine to carcinogenic 2-naphthylamine in rats. Arch Toxicol 87(7):1265–1272. https://doi.org/10.1007/s00204-013-1025-5

Yanez-Sedeno P, Pingarron JM, Riu J, Rius FX (2010) Electrochemical sensing based on carbon nanotubes. Trends Anal Chem 29(9):939–953. https://doi.org/10.1016/j.trac.2010.06.006

Yang Y, Gupta MC, Dudley KL (2007) Towards costefficient EMI shielding materials using carbon nanostructure based nanocomposites. Nanotechnology 18(34):345701. https://doi.org/10.1088/09574484/18/34/345701

Yi Y, Zhu G, Wu X, Wang K (2016) Highly sensitive and simultaneous electrochemical determination of 2- aminophenol and 4-aminophenol based on poly(l-arginine)-β-cyclodextrin/carbon nanotubes@graphene nanoribbons modified electrode. Biosensors Bioelectron 77:353–358. https://doi.org/10.1016/j.bios.2015.09.052